A Cross-Referencing-Based Droplet Manipulation Method for High-Throughput and Pin-Constrained Digital Microfluidic Arrays*

Tao Xu and Krishnendu Chakrabarty
Department of Electrical and Computer Engineering
Duke University, Durham, NC 27708, USA
{tx, krish}@ee.duke.edu

Abstract

Digital microfluidic biochips are revolutionizing high-throughput DNA sequencing, immunoassays, and clinical diagnostics. As high-throughput bioassays are mapped to digital microfluidic platforms, the need for design automation techniques for pin-constrained biochips is being increasingly felt. However, most prior work on biochips CAD has assumed independent control of the underlying electrodes using a large number of (electrical) input pins. We propose a droplet manipulation method based on a "cross-referencing" addressing method that uses "row" and "columns" to access electrodes. By mapping the droplet movement problem to the clique partitioning problem from graph theory, the proposed method allows simultaneous movement of a large number of droplets on a microfluidic array. This in turn facilitates high-throughput applications on a pin-constrained biochip. We use random synthetic benchmarks and a set of multiplexed bioassays to evaluate the proposed method.

1. Introduction

Microfluidics technology has made great strides in recent years [1,2,3]. Promising applications of this emerging technology include high-throughput DNA sequencing, immunoassays, environmental toxicity monitoring, and point-of-care diagnosis of diseases [4]. Microfluidics-based miniaturized devices, often referred to in the literature as biochips, are being increasingly used for laboratory procedures involving molecular biology.

Currently, most commercially-available biochips rely on continuous fluid flow in etched microchannels. Fluid flow is controlled either using micropumps and microvalves [2] or using electrokinetics [5]. An alternative category of microfluidic biochips relies on the principle of electrowetting-on-dielectric. Discrete droplets of nanoliter volumes can be manipulated in a "digital" manner on a two-dimensional electrode array. Hence this technology is referred to as "digital microfluidics" [1].

A digital microfluidic biochip typically consists of a patterned metal electrode array (e.g., chrome or indium tin oxide), on which fluid-handling operations such as merging, splitting, mixing, and dispensing of nano-liter droplets containing biological samples are executed. Electrodes are connected to control pins for electrical activation. A number of prototypes of "digital" biochips use a direct-addressing scheme for the control of electrodes [6]. Each electrode is connected to a dedicated control pin; it can therefore be activated independently. This method allows the maximum freedom of droplet manipulation, but it necessitates an excessive number of control pins for practical biochips. As more bioassays are concurrently executed on digital microfluidic platforms [7,8], system complexity and the number of electrodes is expected to increase steadily. A large number of control pins and the associated interconnect routing problem significantly adds to product cost. Thus, the design of pin-constrained digital microfluidic arrays is of great practical importance for the emerging marketplace.

*This work was supported in part by the National Science Foundation under grants IIS-0312352 and CCF-0541055.

Electrode addressing methods that allow the control of digital microfluidic arrays with a small number of pins are now receiving attention. The method presented in [9] uses array partitioning and careful pin assignment to reduce the number of control pins. However, this method leads to a mapping of pins to electrodes that is specific to a target biofluidic application. An improved design method based on array partitioning is presented in [10] but it is also specific to a given bioassay. A more promising design uses row and column addressing, which is referred to as "cross referencing". An electrode is connected to two pins, corresponding to a row and a column, respectively [11]. However, the cross-referencing method cannot handle more than two arbitrarily-positioned droplets simultaneously due to the problem of electrode interference. This limitation is a major drawback for high-throughput applications, such as DNA sequencing and large-scale proteomic analysis [12].

In this paper, we propose an automated droplet manipulation method and the design of pin-constrained biochips for high-throughput applications. The proposed design is based on the cross-referencing method decribed in [11], but in contrast to [11], it allows multiple droplets to be transported simultaneously. The graph-theoretical concept of clique partitioning is used to determine groups of droplet that can be simultaneously moved on the microfluidic array.

The rest of the paper is organized as follows. Section 2 provides an overview of digital microfluidic biochips. In Section 3, we discuss related prior work on pin-constrained biochip design for high-throughput applications. Section 4 maps the droplet manipulation problem to graph theory and presents a solution that attempts to maximize the throughput for crossing-referencing-based biochips. The proposed method is then evaluated using random synthetic benchmarks in Section 5. A multiplexed bioassay is also used as a case study. Finally, conclusions are drawn in Section 6.

2. Digital Microfluidic Biochips

In this paper, we consider digital microfluidic biochips that rely on the principle of electrowetting-on-dielectric. Droplets of nanoliter volumes, which contain biological samples, are manipulated on a two-dimensional electrode array [1]. A unit cell in the array includes a pair of electrodes that acts as two parallel plates. In most prototype digital microfluidic biochips based on the direct-addressing scheme, the bottom plate contains a patterned array of individually controlled electrodes, and the top plate is coated with a continuous ground electrode. A droplet rests on a hydrophobic surface over an electrode, as shown in Fig. 1. Recently, coplanar microfluidic devices, i.e., arrays without a top plate, have also been demonstrated [13]. Using the electrowetting phenomenon, droplets can be moved to any location on a two-dimensional array. An alternative category of digital microfluidic biochips utilizes orthogonally-placed pin rows on top and bottom plates. A unit cell can be activated by selecting orthogonally positioned pins on top and bottom plate which cross at this cell.

Both designs move droplets by applying a control voltage to a unit cell adjacent to the droplet and, at the same time, deactivating

978-3-9810801-2-4/DATE07 © 2007 EDAA

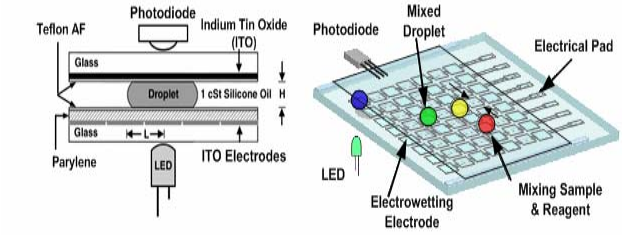

Fig. 1: Schematic diagram of a digital microfluidic biochip.

the one just under the droplet. This electronic method of wettability control creates interfacial tension gradients that move the droplets to the charged electrode. Fluid-handling operations such as droplet merging, splitting, mixing, and dispensing can be executed in a similar manner. For example, mixing can be performed by routing two droplets to the same location and then turning them about some pivot points [14]. The digital microfluidic platform offers the additional advantage of flexibility, referred to as reconfigurability, since fluidic operations can be performed anywhere on the array. Droplet routes and operation scheduling result are programmed into a microcontroller that drives electrodes in the array. In addition to electrodes, optical detectors such as LEDs and photodiodes are also integrated in digital microfluidic arrays to monitor colorimetric bioassays [3].

Demonstrated applications of digital microfluidics include the on-chip detection of explosives such as commercial-grade 2,4,6-trinitrotoluene (TNT) and pure 2,4-dinitrotoluene [6], automated on-chip measurement of airborne particulate matter [15, 16], and colorimetric assays [7]. Digital microfluidic biochips are being designed for on-chip gene sequencing through synthesis [16], protein crystallization, clinical diagnostics for high throughput with low sample volumes, and integrated hematology, pathology, molecular diagnostics, cytology, microbiology, and serology onto the same platform [17]. Recently, a droplet-based biochip that embeds more than 600,000 20 μm by 20 μm electrodes and uses dielectrophoresis for droplet manipulation and control has been demonstrated [18].

In a recent review paper on the use of microfluidics for protein crystallization [19], the following question was posed: can we purchase identical crystallization devices, produced under adequate quality control? The authors go on to say, "Drawing upon integrated circuits as an analogy, microfluidics devices may be reducible to a standard set of discrete operations which can then be custom assembled to form more complex operations as needed. With this approach, the success of manufacturing investment does not have to rest upon a single application." The discrete droplet-based biochip being considered in this paper is perfectly suited as a platform technology, since it avoids the common pitfall of custom devices offered by other continuous-flow microfluidic technologies.

3. Related Prior Work

Recent years have seen a steady increase in the level of integration and system complexity of digital microfluidic biochips [16]. These advances in technology serve as a powerful driver for research on CAD tools for biochip design. Classical architectural and geometric-level synthesis method can be adapted for the automated design of biochips that can execute laboratory protocols [20,21]. A unified synthesis method, which combines operation scheduling, resource binding, and module placement, has been proposed in [20]. Systematic droplet routing strategies have also been developed [21,22,23]. These early design automation techniques are useful for biochip design and rapid prototyping, but they all rely on the availability of a direct-addressing scheme.

Pin-constrained design of digital microfluidic biochips was recently proposed in [9]. This method uses array partitioning and careful pin assignment to reduce the number of control pins. However, it requires detailed information about the scheduling of assay operations, microfluidic module placement, and droplet routing pathways. Thus, the array design in such cases is specific to a target biofluidic application. An improved design method based on array partitioning is presented in [10] but it is also specific to a given bioassay.

In another method proposed in [7], the number of control pins for a fabricated electrowetting-based biochip is minimized by using a multi-phase bus for the fluidic pathways. Every nth electrode in an n-phase bus is electrically connected, where n is small number (typically $n = 4$). Thus, only n control pins are needed for a transport bus, irrespective of the number of electrodes that it contains. Although the multi-phase bus method is useful for reducing the number of control pins, it is only applicable to a one-dimensional (linear) array.

An alternative method based on a cross-reference driving scheme is presented in [11]. This method allows control of an $N \times M$ grid array with only $N+M$ control pins. The electrode rows are patterned on both the top and bottom plates, and placed orthogonally. In order to drive a droplet along the X-direction, electrode rows on the bottom plate serve as driving electrodes, while electrode rows on the top serve as reference ground electrodes. The roles are reversed for movement along the Y-direction, as shown in Fig. 2. This cross-reference method facilitates the reduction of control pins. However, due to electrode interference, this design cannot handle the simultaneous movement of more than two droplets. The resulting serialization of droplet movement is a serious drawback for high-throughput applications.

The minimization of the assay completion time, i.e., the maximization of throughput, is essential for environmental monitoring applications where sensors can provide early warning. Real-time response is also necessary for surgery and neo-natal clinical diagnostics. Finally, biological samples are sensitive to the environment and to temperature variations, and it is difficult to maintain an optimal clinical or laboratory environment on chip. To ensure the integrity of assay results, it is therefore desirable to minimize the time that samples spend on-chip before assay results are obtained. Increased throughout also improves operational reliability. Long assay durations imply that high actuation voltages need to be maintained on some electrodes, which accelerate insulator degradation and dielectric breakdown, reducing the number of assays that can be performed on a chip during its lifetime.

4. Interference-Free Droplet Manipulation Based on Destination-Cell Categorization

In this section, we focus on the problem of manipulating multiple droplets based on digital microfluidic biochips that use cross-referencing to address the electrodes.

4.1 Electrode Interference

For the concurrent manipulation of multiple droplets on a cross-referencing-based biochip, multiple row and column pins must be selected to activate the destination cells, i.e., cells to which the droplets are supposed to move. However, the selected row and column pins may also result in the activation of cells other than the intended droplet destinations. An example is shown in Fig. 3. The goal here is to route Droplets 1, 2, 3 simultaneously to their destination cells. Droplet 4 is supposed to remain in its current location. However, two additional cells are activated unintentionally when the activation voltage is applied to the row and column pins

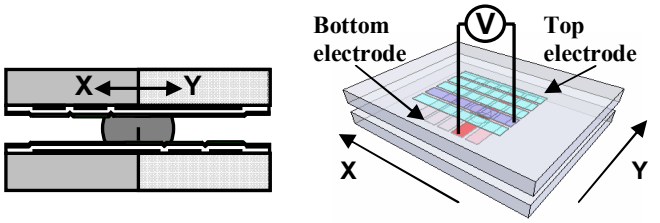

Fig 2: Cross sections of a cross-referencing microfluidic device that uses single-layer driving electrodes on both top and bottom plates.

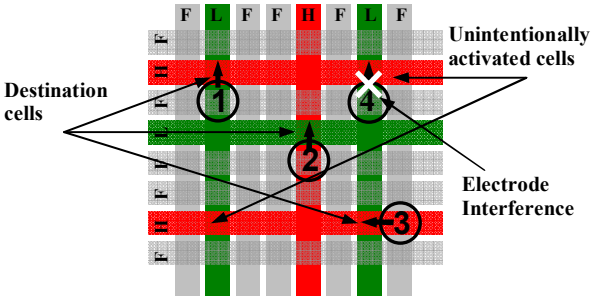

Fig. 3: An example to illustrate the problem of electrode interference. H/L stands for high/low voltage pairs to activate the cells, and unselected row/column pins are left floating (F).

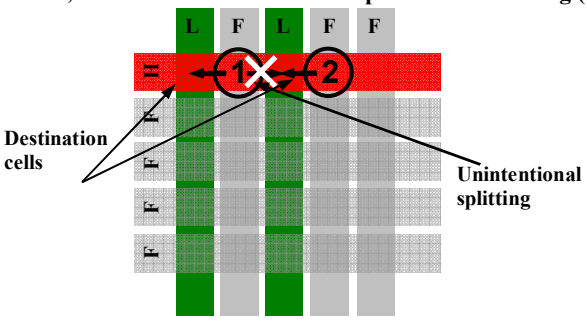

Fig 4: An example of electrode interference within the same row.

corresponding to the destination cells. As a result, Droplet 4 is unintentionally moved one cell up (along the Y-direction). We refer to this phenomenon as electrode interference.

4.2 Destination-Cell Categorization

As shown in Fig. 3, the concurrent manipulation of multiple droplets must be carried out without introducing any electrode interference. Here we propose a solution based on destination-cell categorization. Note that the problem highlighted in Fig. 3 can be avoided if the destination cells of the droplets being moved simultaneously reside on the same column or row. However, electrode interference may still occur within the same column or row, as shown in Fig. 4.

Suppose Droplet 1 and Droplet 2 are both moved one cell to the left at the same time. Even though no additional cells are activated unintentionally, Droplet 1 undergoes unintentional splitting in this situation. Fortunately, this problem can be avoided by satisfying the fluidic constraints described in [21]. These constraints are given by the following set of inequalities: (i) $|P_i(t)-P_j(t)| \geq 2$; (ii) $|P_i(t+1)-P_j(t)| \geq 2$; (iii) $|P_i(t)-P_j(t+1)| \geq 2$; (iv) $|P_i(t+1)-P_j(t+1)| \geq 2$, where $P_i(t)$ is the position of droplet i at time t and $P_j(t)$ is the position of droplet j at time t.

The fluidic constraints avoid unintentional fluidic operations that arise due to the overlapping of droplets over adjacent electrodes. Thus they apply to both direct-addressing-based and

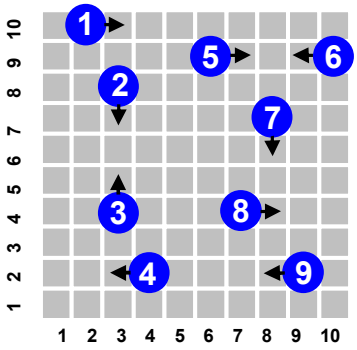

Fig. 5: Example to illustrate destination-cell-based categorization.

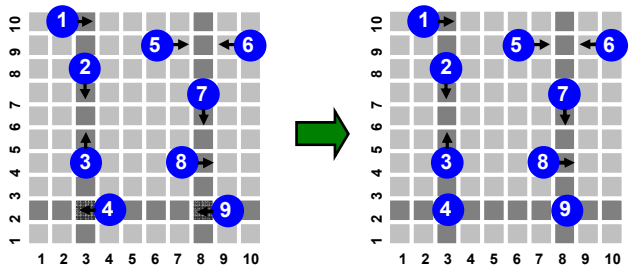

Fig. 6: Example to illustrate the concurrent movement of a group of droplets.

cross-referencing-based biochips. In Fig. 4, the intended multiple droplet manipulation violates the constraint $|P_i(t+1)-P_j(t)| \geq 2$. If the fluidic constraints are satisfied at all times, it is safe to carry out concurrent manipulation of multiple droplets whose destination cells are accessed by the same column or row.

On the basis of the above observations, we consider the droplets that can be moved simultaneously as part of the bioassay, and place them in different groups. A group consists of droplets whose destination cells share the same column or row. An example is shown in Fig. 5. A total of nine droplets are needed to be moved on a 10×10 array. As discussed above, we group the droplet movements according to their destination cells. For example, Droplets 4 and 9 from a group since the destination cells in both cases resides on Row 2. Similarly Droplets 1, 2, and 3 are placed in the same group since they are all moving to Column 3. Following this grouping process, we finally get four groups of droplets, i.e., {4,9}, {1,2,3}, {5,6}, {7,8}.

In this way, the manipulation of multiple droplets is ordered in time; droplets in the same group can be moved simultaneously without electrode interference, but the movements for the different groups must be sequential. For example, droplet movements for the group {4,9} in Fig. 5 can be carried simultaneously, as shown in Fig. 6. Droplet movements are carried out one group after another until all the droplet movements are completed.

Note that the ordering of droplet movements based only on the above grouping strategy can cause electrode interference and inadvertent mixing. An example is shown in Fig. 7. The movement of Droplet 2 alone to the left by activating Column 3 will not influence Droplet 1. Similarly, the movement of Droplet 1 alone to the right by activating Column 2 will not influence Droplet 2. However, if these two droplets are moved concurrently, as determined by the grouping procedure, by the activation of (Column 2, Row 2) and (Column 3, Row 2), they mix at (3,2). However, manipulations of this type violate the fluidic constraint given by

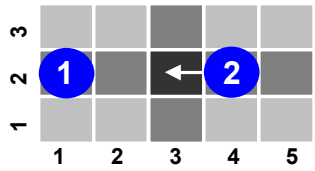

Fig. 7: Example of electrode interference due to asynchronous processing of multiple droplet manipulations.

$|P_i(t+1)-P_j(t+1)| \geq 2$. Therefore, such problems can be avoided if the grouping procedure incorporates the fluidic constraints.

Although the grouping of droplets based on destination cells reduces the number of droplets that can be simultaneously moved, this approach provides more concurrency than the baseline method of moving one droplet at a time. Compared to direct-addressing, an order of magnitude reduction in the number of control pins is obtained. Simulation results in Section 6 show that there is only a small increase in the bioassay processing time compared to direct-addressing.

4.3. Graph-theoretic model and clique partitioning

We have thus far introduced the basic idea of multiple droplet manipulations based on destination-cell categorization, and shown that the droplets in each group can be moved simultaneously. Assuming that each step takes constant processing time, the total completion time for a set of droplet movement operations is determined by the number of groups derived from the categorization of destination cells. Note however that the grouping need not be unique. For instance, in the example of Fig. 5, we can form four groups, i.e., {4,9}, {1,2,3}, {5,6} and {7,8}. However, {1,2,3,4},{5,6},{7,8,9} is also a valid grouping of the droplets. The latter grouping is preferable because three groups allow more concurrency, and therefore lower bioassay completion time.

The problem of finding the minimum number of groups can be directly mapped to the clique partitioning problem from graph theory [24]. To illustrate this mapping, we use the droplet manipulation problem defined in Fig. 5. Based on the destinations of the droplets, an undirected graph, referred to as the droplet movement graph, is constructed for each time-step; see Fig. 8. Each node in the droplet movement graph represents a droplet. An edge in the graph between a pair of nodes indicates that the destination cells for the two droplets either share a row or a column. For example, Nodes 1 and 2, which represent the Droplet 1 and Droplet 2, respectively, are connected by an edge because the destination cells for these droplets are accessed using Column 3 in the array. Similarly, Nodes 4 and 9 are connected by an edge because the corresponding destination cells are addressed using the same row.

A clique in a graph is defined as a complete subgraph, i.e., any two nodes in this subgraph are connected by an edge [24]. Clique partitioning refers to the problem of dividing the nodes into overlapping subsets such that the subgraph induced by each subset of nodes is a clique. A minimal clique partition is one that covers the nodes in the graph with a minimum number of non-overlapping cliques. The grouping of droplets as discussed above is equivalent to the clique partitioning problem. The categorization of destination cells using the grouping of droplets is equivalent to the problem of determining a minimal clique partition. Cliques of different sizes for a given droplet movement graph are shown in Fig. 8. A minimal clique partition here is given by {1,2,3,4}, {5,6}, {7,8,9}, which corresponds to the groups derived above. Even though the general clique partitioning problem is known to be NP-hard [25], a number of heuristics are available in the literature to solve it in an efficient manner.

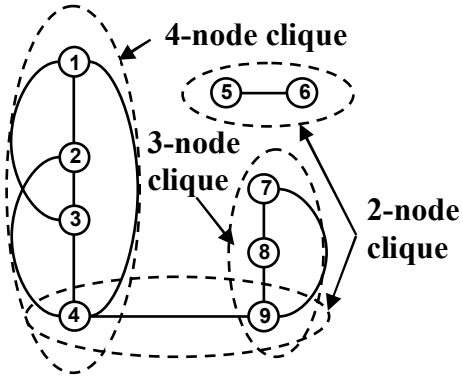

Fig. 8: Mapping destination cell layout to undirected graph

4.4. Algorithm for Droplet Grouping

Next we describe a greedy algorithm to determine a (minimal) clique partition for the droplet movement graph (DMG). The algorithm determines cliques for the DMG in an iterative manner.The largest clique is first determined and then nodes and edges corresponding to this clique are deleted form the graph. Next, the clique searching procedure is applied to the reduced graph. The algorithm terminates when all the nodes in the DMG have been deleted, i.e., an empty graph is obtained. The computational complexity of this problem for the DMG is linear in the number of rows/columns. Recall that the cliques can only be formed among nodes sharing the same row or column. Therefore, the largest clique can be determined the scanning the columns and rows of the array. Thus a maximum of only $N+M$ iterations are needed for the droplet movement graph derived from an $N \times M$ array.

Note that even though in each step of the above algorithm, the largest clique and the associated destination cells are deleted, the absence of the corresponding destination cells does not lead to any added complexity for droplet movement. This is because the droplet movements involving these destination cells are incorporated in the clique determined at this step. Therefore, when the algorithm terminates with an empty graph, all droplet movements have been processed without any electrode interference.

The steps of the complete procedure to determine the order of droplet movements can be stated as follows:

1. Obtain the required droplet movements (from a synthesis tool such as [21]), and organize these movements in the form of snapshots corresponding to different time-steps. The fluidic constraints described in Section 4.3 need to be satisfied for each snapshot.
2. Compare consecutive snapshots to determine the destination cells for the droplets.
3. Scan each row and each column to find the row/column with the largest set of destination cells. The destination cells thus determined forms a group of droplets that can be simultaneously moved. If no row/column contains more than one destination cells, set the flag END to 1.
4. If END = 1, process the remaining movements in multiple steps, but with two droplets at each step. Else carry out the droplet movements indicated by Step 3.
5. Check if all the movements in the snapshot have been processed. If the check yields a negative outcome, repeat Step 3.
6. Check whether all the snapshots are processed. If not, get the next snapshot and repeat Step 2, else terminate the procedure.

5. Evaluation and Simulation Results

In this section, we use random synthetic benchmarks and a set of multiplexed bioassays to evaluate the proposed method.

5.1 Random Synthetic Benchmarks

We first use random synthetic benchmarks to evaluate the effectiveness of the proposed droplet movement approach. Digital microfluidic arrays of size $N \times N$, (N = 25, 50, 75) are considered here. For each array, we consider 1000 simulated droplet movement plans. Each droplet movement plan is defined by a starting snapshot and destination snapshot. The starting snapshot is generated by injecting a droplet in the array with probability k, referred to as the droplet injection probability (DIP). A special check is incorporated in the generation process to avoid the violation of fluidic constraints. Results derived from this process can be viewed as snapshots of droplets moving around the chip. Each droplet movement plan is provided as input to the proposed method and the number of steps required for droplet movement is calculated. One-at-a-time droplet movement is also considered and the results are recorded for the purpose of comparison.

To evaluate the proposed method, we introduce the parameter "number-of-steps-ratio" (NSR), defined by the equation NSR = N_p/N_o, where N_p (N_o) is the number of movement steps for the proposed method (one-at-a-time baseline method). Small values of NSR are clearly desirable. We calculate the NSR values for different array sizes and the results are as shown in Table 1.

As shown Table 1, regardless of DIP value, the NSR decreases with array size. This shows that the proposed method is more efficient for concurrent droplet manipulation on large-scale digital microfluidic arrays. For a given array size, the proposed method achieves lower NSR values for higher values of DIP. Thus we see that compared to the one-at-a-time scheme, droplets can be manipulated more efficiently for high-throughput biochips with higher concurrency in biochip operations.

5.2 A Multiplexed Bioassay Example

We next consider a real-life application, namely a multiplexed biochemical assay consisting of a glucose assay and a lactate assay based on colorimetric enzymatic reactions, which have been demonstrated recently [3]. Fig. 9 shows the flowchart for the multiplexed assays in the form of a sequencing graph [26]. For each sample or reagent, two droplets are dispensed into the array. Four pairs of droplets, i.e., $\{S_1, R_1\}$, $\{S_1, R_2\}$, $\{S_2, R_1\}$, $\{S_2, R_2\}$ are routed together in sequence for the mixing operation. Mixed droplets are finally routed to detection site for analysis. In [7], the multiplex bioassays were mapped to a digital microfluidic platform containing a 15×15 array, as shown in Fig. 10. A depiction of the droplet pathways for multiplexed glucose and lactase assays is given in Fig. 10.

For simplicity, we ignore the mixing and detection operations and focus on the dispensing of droplets and their transportation to the mixer. We refer to these steps as the droplet transportation steps of the bioassay. As a baseline, we first transport droplets by moving only one droplet at a time. Recall that two droplets must be dispensed and routed to the mixer for each sample or reagent, therefore the total time required is simply the sum of times needed to transport each droplet. A total of 8 droplets must be transported at the rate of 0.33 seconds/droplet, hence the total transportation time is 35 seconds. Next we assume that the array is controlled using a using direct-addressing scheme with 225 control pins. In this case, droplets can be moved concurrently on the array and the dispensing and routing operation take only 7 seconds.

Finally, we apply the proposed droplet manipulation method based on clique partitioning to the example of multiplexed bioassays. The droplet positions for the different time-steps that we consider here correspond to the succession of droplet positions obtained using the direct-addressing method. Note that the transition between two time-steps, which takes only one manipulation step for direct addressing, can sometimes be carried out in one time-step for the proposed cross-referencing-based method as well. No additional droplet manipulation steps are needed in such cases. For other cases, the proposed method decomposes a single droplet movement step, which is adequate for direct addressing, into a succession of steps determined using destination-cell-based categorization. An example is shown in Fig. 11-12.

In the manipulation step in Fig. 11, 8 droplet movements, i.e., 4 dispensing and 4 droplet transportation operations, are to be executed simultaneously. When the proposed cross-referencing based method is applied, the 8 movements are categorized into two groups and implemented with two manipulation steps, as shown in Fig. 12(a) and Fig. 12(b), respectively.

In this manner, the proposed droplet manipulation method is applied to every time-step derived from the direct-addressing scheme, and results in a completion time of 15 seconds. We therefore obtain a significant reduction in the assay completion time compared to the one-at-a-time baseline method. This improvement

Table 1: Random synthetic benchmarks, sample size = 1000.

DIP	Array Size	NSR
0.1	25×25	0.31
0.1	50×50	0.24
0.1	75×75	0.19
0.15	25×25	0.28
0.15	50×50	0.20
0.15	75×75	0.14

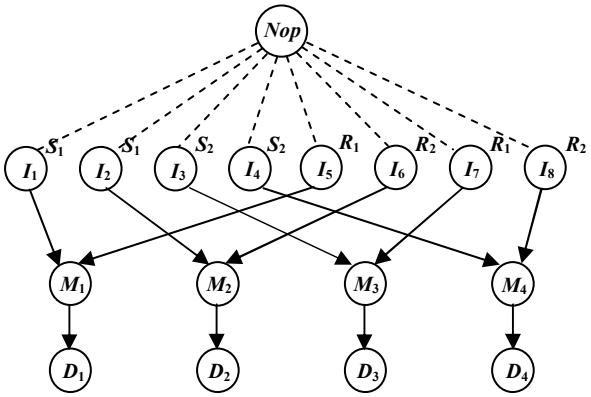

Fig. 9: Sequencing graph model for a multiplexed *in-vitro* diagnostics. S_1, S_2 are samples, R_1, R_2 are reagents, M_1, M_2, M_3, M_4 are mixing operations, and *Nop* is a dummy source node.

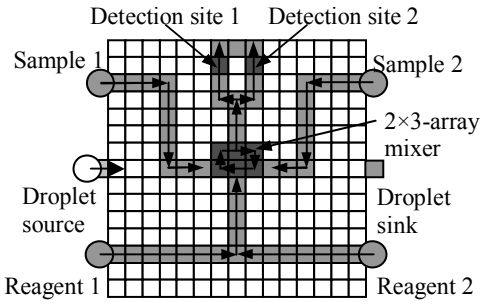

Fig. 10: A 15×15 array used for multiplexed bioassays.

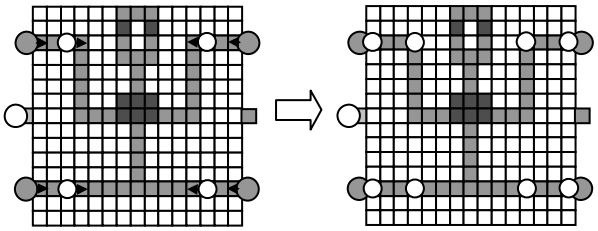

Fig. 11: A manipulation step in direct-addressing routing.

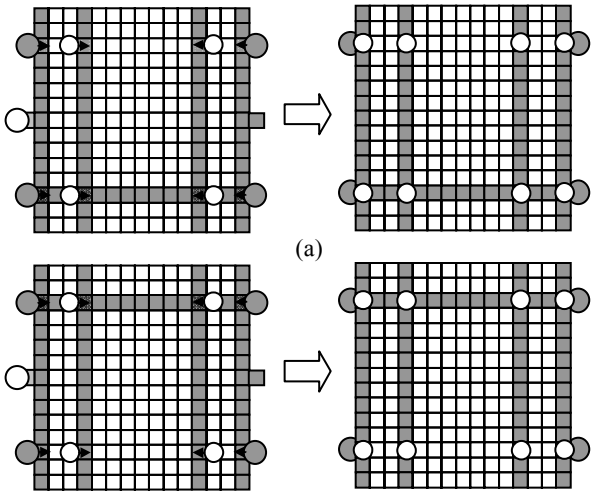

Fig. 12: Implementing the step in Fig. 11 by two substeps using the proposed cross-referencing based method: (a) Substep 1; (b) Substep 2.

is even more significant if we consider the fact that for the one-at-a-time droplet manipulation method, droplet routing can be carried out while mixing is being carried at some place on the array. Moreover, if multiple copies of the same modules, e.g., the one shown in Fig. 9, are placed in parallel on the array, which is a very common "regularization" strategy in VLSI design, the droplet movement time using the proposed method is not affected. In contrast, the one-at-a-time manipulation method results in an *n*-fold increase in the assay completion time if *n* copies of the module in Fig. 9 are mapped to the array. Note that the completion time obtained using the proposed droplet manipulation method is slightly more than that for direct-addressing method (15 seconds versus 7 seconds). However, the proposed method requires only 30 (15+15) control pins while 225 (15×15) pins are required for the direct-addressing method.

6. Conclusions

We have proposed a droplet manipulation method for a "cross-referencing" addressing method that uses "rows" and "columns" to access electrodes in digital microfluidic arrays. By mapping the droplet movement problem to the clique partitioning problem from graph theory, the proposed method allows simultaneous movement of a large number of droplets. A linear-time heuristic algorithm based on row-scanning and column-scanning has been used to derive the clique partitions. We have use random synthetic benchmarks and a set of multiplexed bioassays to evaluate the proposed method. Results show that high throughput can be obtained using a small number control pins. This work will allow bioassays for high-throughput sequencing, immunoassays, and clinical diagnostics to be mapped to pin-constrained and low-cost biochips, and simplify the design and implementation of such biochips.

References

[1] R. B. Fair et al., "Electrowetting-based on-chip sample processing for integrated microfluidics", *Proc. IEDM*, pp. 32.5.1-32.5.4, 2003.

[2] E. Verpoorte and N. F. De Rooij, "Microfluidics meets MEMS", *Proc. IEEE*, vol. 91, pp. 930-953, 2003.

[3] J. Zeng and T. Korsmeyer, "Principles of droplet electrohydrodynamics for lab-on-a-chip", *Lab on a Chip*, pp. 265-277, 2004.

[4] T. H. Schulte et al., "Microfluidic technologies in clinical diagnostics", *Clinica Chimica Acta*, vol. 321, pp. 1-10, 2002.

[5] Y. Wang et al., "Composable Behavioral Models and Schematic-Based Simulation of Electrokinetic Lab-on-a-Chip Systems", *IEEE TCAD*, vol. 25, pp. 258-273, February 2006.

[6] R.B. Fair et al., "Integrated chemical/biochemical sample collection, pre-concentration, and analysis on a digital microfluidic lab-on-a-chip platform", *Lab-on-a-Chip*: *Platforms, Devices, and Applications, Conf.* 5591, SPIE Optics East, 2004.

[7] V. Srinivasan et al., "An integrated digital microfluidic lab-on-a-chip for clinical diagnostics on human physiological fluids", *Lab on a Chip*, vol. 4, pp. 310-315, 2004.

[8] V. Srinivasan et al., "Clinical diagnostics on human whole blood, plasma, serum, urine, saliva, sweat, and tears on a digital microfluidic platform", *Proc. μTAS*, pp.1287-1290, 2003.

[9] W. Hwang et al., "Automated design of pin-constrained digital microfluidic arrays for lab-on-a-chip applications", *Proc. IEEE/ACM DAC*, pp. 925-930, 2006.

[10] T. Xu and K. Chakrabarty, "Droplet-trace-based array partitioning and a pin assignment algorithm for the automated design of digital microfluidic biochips", *IEEE/ACM CODES+ISSS*, pp. 112-117, 2006.

[11] S. K. Fan et al., "Manipulation of multiple droplets on N×M grid by cross-reference EWOD driving scheme and pressure-contact packaging", *Proc. IEEE MEMS Conf.*, pp. 694-697, 2003.

[12] H. Moon et al., "Integrated digital microfluidic chip for multiplexed proteomic sample preparation and analysis by MALDI-MS", *Lab on a Chip*, vol. 6, pp. 1213-1219, 2006.

[13] P. Y. Paik et al., "Coplanar digital microfluidics using standard printed circuit board processes", *Proc. μ*TAS, pp. 566-568, 2005.

[14] P. Y. Paik et al., "Rapid droplet mixers for digital microfluidic systems", *Lab on a Chip*, vol. 3, pp. 253-259, 2003.

[15] Y. Zhao and S. K. Cho, "Microparticle sampling by electrowetting-actuated droplet sweeping", *Lab on a Chip*, vol. 6, pp. 137-144, 2006.

[16] R. B. Fair et al., "Chemical and biological applications of digital microfluidic devices", accepted for publication in *IEEE Design & Test of Computers*, 2006.

[17] Avanced Liquid Logic, Inc., http://www.liquid-logic.com

[18] Silicon Systems, http://www.siliconbiosystems.com

[19] M. van der Woerd et al., "The promise of macromolecular crystallization in microfluidic chips", *Journal of Structural Biology*, vol. 142, pp. 180-187, 2003.

[20] F. Su and K. Chakrabarty, "Unified high-level synthesis and module placement for defect-tolerant microfluidic biochips", *Proc. DAC,* pp. 825-830, 2005.

[21] F. Su et al., "Droplet routing in the synthesis of digital microfluidic biochips", *Proc. DATE Conference*, pp. 323-328, 2006.

[22] K. F. Böhringer, "Modeling and controlling parallel tasks in droplet-based microfluidic systems", *IEEE TCAD*, vol. 25, pp. 329-339, 2006.

[23] E. J. Griffith et al., "Performance characterization of a reconfigurable planar array digital microfluidic system", *IEEE TCAD*, vol. 25, pp. 340-352, 2006.

[24] J. L. Gross and J. Yellen, *Graph Theory and Its Applications*, CRC Press, FL, 1999.

[25] M. R. Garey and D. S. Johnson, *Computers and Intractability: A Guide to the Theory of NP-Completeness*, W. H. Freeman & Co., CA, 1979.

[26] F. Su and K. Chakrabarty, "Architectural-level synthesis of digital microfluidics-based biochips", *Proc. IEEE ICCAD*, pp. 223-228, 2004.